AGU PUBLICATIONS

Water Resources Research

RESEARCH ARTICLE
10.1002/2014WR016631

On kinematics and flow velocity prediction in step-pool channels

V. D'Agostino[1] and T. Michelini[1]

[1]Department of Land, Environment, Agriculture and Forestry, TESAF Dep., Università degli Studi di Padova, Legnaro, Padova, Italy

Key Points:
- The flow velocities in three step-pool reaches were measured to assess the average reach velocity
- An empirical relationship to predict the energy loss from the step crest to pool end was calibrated
- A formula, based on relative submergence and slope, was found to calculate Manning's *n* coefficient

Correspondence to:
V. D'Agostino,
vincenzo.dagostino@unipd.it

Citation:
D'Agostino, V., and T. Michelini (2015), On kinematics and flow velocity prediction in step-pool channels, *Water Resour. Res.*, *51*, 4650–4667, doi:10.1002/2014WR016631.

Received 5 NOV 2014
Accepted 17 MAY 2015
Accepted article online 21 MAY 2015
Published online 28 JUN 2015

Abstract This paper verifies methods for the prediction of mean flow velocity at the reach scale in mountain streams, investigating the kinematics of a series of two small-scale artificial step-pool sequences and a transitional reach between plane-bed and step-pool under well-controlled hydraulic conditions, and improving the estimation of the energy expenditure between the step crest and the downstream pool. Experimental data were collected using three fish ladder reaches with slopes between 2.6 and 10%. Four types of field measurements were conducted: topographical surveys to extract the thalweg profiles and cross-sectional geometry of reference cross sections; grain size analyses of the bed surface; steady state runs with a given flow rate (0.005–0.234 m^3/s), and surveying of the water profile in the most significant cross sections. The following main conclusions were reached: (i) the dominance of spill resistance at the lowest discharge (pool water depth-step height ratios of 0.4) causes primary dimensionless head losses of up to 80%, and these losses progressively decrease to approximately 40% when the water discharge and related pool water depth submerge the upstream step height. A specific predictive equation for the head loss was calibrated and then verified via data from the Rio Cordon. (ii) The verification of literature-sourced equations to predict the reach-averaged flow velocity provided suitable results for several of these equations indicating that the use of a specific step-pool equation does not appear to be crucial to achieving accurate predictions.

1. Introduction

Steep mountain streams have irregular beds, and the mean flow velocity is strongly affected by the coarsest bed sediments and by their arrangement in the form of steps, pools, cascades, and rapids. Precise knowledge of the flow behavior of steep streams is mandatory for hydraulic and hydrological modeling [*Abrahams et al.*, 1995; *Modrick and Georgakakos*, 2014], stream restoration design [*Lenzi et al.*, 2000], geomorphic analysis [*Chin*, 2003], and ecological studies [*Yochum et al.*, 2012]. The assessment of the mean velocity depends on the main components of the flow resistance: grain, form, and spill resistance. Grain energy losses are caused by the skin friction drag of the bed particles as a whole [*Einstein and Barbarossa*, 1952; *Parker and Peterson*, 1980]. Form and spill resistance represent local energy losses caused by interactions between the flow and channel boundary and are generated by macroroughness elements and obstructions, such as grain clusters, bed/banks forms, large woody debris, and vegetation [*MacFarlane and Wohl*, 2003; *David et al.*, 2011]. In step-pool, rapid and cascade reaches, which are very common in alpine torrents [*D'Agostino*, 2005], spill resistance is typically dominant [*Kaufmann*, 1987; *Curran and Wohl*, 2003; *MacFarlane and Wohl*, 2003; *Wilcox et al.*, 2006; *Kaufmann et al.*, 2008; *Comiti et al.*, 2009], even though the spill resistance is partly reduced during high flows [*David et al.*, 2010, 2011].

Alluvial mountain rivers with thalweg gradients between 0.03 and 0.20 m/m may form step-pool sequences, which are characterized by large-scale roughness [*Montgomery and Buffington*, 1997]. The sequences dissipate flow energy due to the stepped longitudinal topography and alternation of the coarsest (steps) and finest (pool) particles [*Keller and Swanson*, 1979; *Montgomery and Buffington*, 1997; *Chin and Wohl*, 2005; *Church and Zimmermann*, 2007]. These morphological units are able to almost maximize the energy losses due to the high flow resistance they generate [*Whittaker and Jaeggi*, 1982; *Abrahams et al.*, 1995]. The analogies between step-pool/rapid sequences and engineered structures [e.g., consolidation check dams, bed sills, grade control structures, and ramps] have motivated investigations of naturally steep channels [*Chin et al.*, 2009]. Steps contribute to the reduction of the mean energy slope mainly through the vertical flow drop that promotes a tumbling flow regime [*Peterson and Mohanty*, 1960] with a critical or supercritical jet

flow over the step lip and subcritical dissipative flow in the pool [*Zimmermann and Church*, 2001; *Wohl and Thompson*, 2000]. Such a flow alternation, which improves the river habitat, water quality, and landscape, has encouraged the artificial imitation of the step-pool morphology in river restoration projects and step stream stabilization works in environmentally sensitive mountain areas [*Lenzi et al*., 2000; *Chin*, 2003; *Curran and Wohl*, 2003; *MacFarlane and Wohl*, 2003].

Given water depth and energy gradient in a prismatic channel, the mean flow velocity depends on the hydraulic resistance of the channel, which can be expressed using Chézy's (C) [1769, in *Chow*, 1973, p. 93], or Darcy-Weisbach's friction factor (f) [1854–1845, in *Chow*, 1973, p. 8] or Manning's roughness coefficient (n) [1889, in *Chow*, 1973, p. 98–99] and, accordingly, the relative normal depth equations. Techniques predicting flow resistance coefficients from field data exist for Chézy's C [e.g., *ASCE Task Force*, 1963], Darcy-Weisbach's f [*Bathurst*, 1985; *Kaufmann*, 1987; *Comiti et al*., 2007; *Kaufmann et al*., 2008], and Manning's n [*Jarrett*, 1984; *Rickenmann*, 1994]. Furthermore, methods to directly estimate mean flow velocity do not consider the classical hydraulic resistances (C, f, n) in mountain rivers. They have been developed using field data [*Jarrett*, 1984; *Rickenmann*, 1994; *Ferguson*, 2007; *Comiti et al*., 2007], laboratory data from self-formed steps [*Aberle and Smart*, 2003; *Comiti et al*., 2009; *Zimmermann*, 2010] and the combination of field data with flume experiments [*Lee and Ferguson*, 2002]. The mean flow velocity has proved to be inversely related to flow resistance [*Limerinos*, 1970; *Bathurst*, 1985; *Lee and Ferguson*, 2002; *Wilcox and Wohl*, 2007; *Reid and Hickin*, 2008; *Ferguson*, 2010], but its expeditious and precise quantification in boulder bed torrents still remains a challenge, particularly in terms of the overall kinematics of a series of step-pool sequences [*David et al*., 2010]. In fact, literature equations for the estimation of resistance in lower-gradient streams generate substantial errors when applied to step-pool and other steep channels [*Bathurst*, 1985; *Marcus et al*., 1992; *Millar*, 1999; *Curran and Wohl*, 2003; *MacFarlane and Wohl*, 2003], particularly in the case that only grain size is used to quantify the bed roughness [*David et al*., 2010, *Yochum et al*., 2012, 2014].

According to literature findings [e.g., *Rickenmann*, 1994; *D'Agostino*, 2005], the mean flow velocity is dependent on the water discharge (Q) or unit discharge (q), channel slope (S), and a reference grain-size variable (D_c). Several approaches use dimensionless hydraulic geometry terms to develop the analysis over a wide range of channel sizes and hydraulic conditions. *Judd and Peterson* [1969] argued that whereas flow in steep streams is locally nonuniform and unsteady, it is macroscopically uniform within a reach. Therefore, a spatially reach-averaged velocity (U) should be predictable from the depth, slope, and one or more resistance parameters representing the statistically averaged effects of form and spill drags [*Lee and Ferguson*, 2002].

For the field study of very rough (maximum sediment diameters > 0.3 m) and narrow streams (bankfull widths < 5 m), a water discharge (Q) measurement is usually more accurate than a flow depth measurement because the irregular bed topography makes the assessment of a representative and precise flow depth difficult [*Rickenmann and Recking*, 2011]. Accordingly, many researchers have calibrated experimental equations to directly predict U [e.g., *Jarrett*, 1984; *Rickenmann*, 1994; *Ferguson*, 2007; *Comiti et al*., 2007]. In a dimensionally correct form, the direct relationship can be written as follows [*Rickenmann*, 1991; *Aberle and Smart*, 2003]:

$$U \propto g^{0.20}\ S^{0.20} q^{0.60} D_c^{-0.40} \tag{1}$$

where q is the unit discharge, D_c is the reference grain diameter or reference geometric bed roughness, and g is the gravity acceleration.

Rickenmann [1991] suggested assuming $D_c = D_{90}$ (the diameter at which 90% of the passing diameters are finer). In contrast, *Aberle and Smart* [2003] and *Zimmermann* [2010] adopted the standard deviation of the longitudinal bed profile (σ_z), the results of which are more significant in streams with substantial bed forms. *Comiti et al*. [2007] introduced the classical hydraulic geometry equation in a dimensionless form:

$$U^* = a\ q^{*m} \tag{2}$$

where a and m are two empirical parameters, and:

$$U^* = \frac{U}{\sqrt{g\ D_c}} \tag{3}$$

$$q^* = \frac{q}{\sqrt{g\ D_c{}^3}}. \tag{4}$$

Table 1. Flow Velocity Prediction Equations Tested in This Study[a]

Author	Equation	
Matakiewickz [1932, in *Indri*, 1942]	$U=2.38\ Rh^{0.70}$	(8)
Jarrett [1984]	$U=3.17\ Rh^{0.83}\ S^{0.12}$	(9)
Bathurst [1985]	$U=(g\ Rh\ S)^{0.5}\ [5.62\log(Rh/D_{84})+4]$	(10)
Rickenmann [1991]	$U=1.3\ g^{0.20}\ S^{0.20}\ q^{0.60}\ D_{90}^{-0.40}$	(11)
Rickenmann [1994]	$U=0.37\ g^{0.33}\ S^{0.20}\ Q^{0.34}\ D_{90}^{-0.35}$	(12)
Aberle and Smart [2003]	$U=0.96\ g^{0.20}\ S^{0.20}\ q^{0.60}\ \sigma_z^{-0.40}$	(13)
D'Agostino [2005]	$U=1.42\ q^{0.48}$	(14)
Comiti et al. [2007] ($D_c=D_{84}$)	$U^*=0.74\ q^{*0.59}\left(\frac{\Delta Z/L_{ss}}{S}\right)^{0.52}$	(15)
Ferguson [2007] ($D_c=D_{84}$)	$U^*=1.44\ q^{*0.60}\ S^{0.2}$	(16)
Comiti et al. [2009] ($D_c=D_{84}$)	$U^*=1.24\ q^{*0.83}$	(17)
Zimmermann [2010] ($D_c=\sigma_z$)	$U^*=0.58\ q^{*0.39}$	(18)
Rickenmann and Recking [2011] ($D_c=D_{84}$)	$U^{**}=1.5471\ q^{**0.7062}\left[1+\left(\frac{q^{**}}{10.31}\right)^{0.6317}\right]^{-0.4930}$	(19)
Yochum et al. [2012]a ($D_c=\sigma_z$)	$U^{**}=q^{**0.16}$	(20)
Yochum et al. [2012]b ($D_c=\sigma_z$)	$U^{**}=0.9\ \left(\frac{d_m}{\sigma_z}\right)^{0.16}$	(21)

[a]Variables: Rh = hydraulic radius (m); d_m = hydraulic depth (m); $\Delta Z/L_{ss}$ = step height-length ratio (-); σ_z = standard deviation of the residuals of a thalweg longitudinal profile regression (m); D_{xx} (diameter for which the xx% of the sieve diameter is finer) (see text and Figure 2 for the other symbols).

Ferguson [2007] and *David et al.* [2010] noted that equation (4) performs better than other equations because q^* is a more powerful predictor than the flow depth (d) over grain size ratio (d/D_c, relative submergence) and is less affected by measurement errors. Recently, *Rickenmann and Recking* [2011] added the slope as a predictive variable in the dimensionless equation:

$$U^{**}=\frac{U}{\sqrt{g\ S\ D_c}} \tag{5}$$

$$q^{**}=\frac{q}{\sqrt{g\ S\ {D_c}^3}} \tag{6}$$

These authors also formulated a hydraulic-geometry-type equation in dimensionless terms:

$$U^{**}=a\ q^{**m} \tag{7}$$

The authors calibrated equation (7) using a data set of 2890 field measurements. They divided the result into three different domains of q^{**} ($q^{**}\geq 100$; $1\leq q^{**}<100$; and $q^{**}<1$). To obtain a smoother transition for the velocity predictions between the three domains, the authors used the logarithmic matching technique proposed by *Guo* [2002]. Certain additional quantitative methods used to predict U in high-gradient channels are listed in Tables 1 and 2, which also contain some pioneering formulas [*Matakiewickz*, 1932 in *Indri*, 1942; *Jarrett*, 1984; *Bathurst*, 1985] focused on the hydraulic behavior of boulder bed torrents.

The hydraulic behavior of a stepped structure like a drop [*Rajaratnam and MacDougall*, 1983] and a ramp [*Pagliara and Chiavaccini*, 2006] have been very accurately investigated and solved. Instead, addressing the natural diversity of the step-pool channels is still partly lacking [*Church and Zimmermann*, 2007], because their full interpretation needs to extend the understanding of a single step/riffle-step pool to a structured continuous sequence of step pools. Furthermore, the uncertainties are more manifest if the overall kinematic behavior of the sequence at different flow stages is under investigation, e.g., to achieve a robust and not too complicated estimation for practical design/restoration purposes. This research aims (i) to verify the

Table 2. Field of Applicability of the Equations in Table 1

Author	Field/Flume	Morphology	Slope	Sample Size[a]
Matakiewickz [1932, in Indri, 1942]	Field	Mountain streams	> 1.6%	-
Jarrett [1984]	Field	Wide range in steep channel	0.2%–3.4%	75
Bathurst [1985]	Field	Gravel and boulder-bed rivers	0.4%–3.7%	44
Rickenmann [1991]	Flume	Run with solid transport	5.0%–20.0%	-
Rickenmann [1994]	Field	Wide range in steep channel	0.8%–63.0%	217
Aberle and Smart [2003]	Flume	Run	2.0%–9.8%	94
D'Agostino [2005]	Field	Mountain streams	0.2%–4.5%	178
Comiti et al. [2007]	Field	Predominantly step-pool	8.0%–21.0%	44
Ferguson [2007]	Field	Wide range in steep channel	0.7%–21.0%	376
Comiti et al. [2009]	Flume	Nappe and skimming flow regime	8.4%–14.0%	205
Zimmermann [2010]	Flume	Step-pool	3.0%–23.0%	139
Rickenmann and Recking [2011]	Field	Wide range in gravel-bed river	0.4%–24.0%	2890
Yochum et al. [2012]a	Field	Step-pool and cascade	5.0%–61.0%	103
Yochum et al. [2012]b	Field	Step-pool and cascade	5.0%–61.0%	78

[a]Number of reaches or tests (for field and flume experiments respectively) investigated by the Authors to derive the empirical equations listed in Table 1.

Figure 1. Photos of (a) *TA* step-pool reach; (b) *TB* step-pool reach; and (c) *TS* transitional reach between plane-bed and step-pool.

above-cited methods for *U* prediction by investigating the kinematic behavior of a series of small-scale artificial step-pool sequences under well-controlled hydraulic conditions and (ii) to refine the prediction of the energy dissipation between the step head and pool end because this, as the mirror of the spill resistance, is of primary importance in the hydraulic modeling of the step-pool reaches and, as a consequence, in the real determination of *U* at the step-pool sequence scale.

2. Material and Methods

Experimental data were collected from two fish ladders (Figure 1) next to the Vanoi torrent (Trento Province, north-eastern Italy). The fish ladders were built to replicate the step-pool morphology and reestablish the river continuum. After an extreme flood occurred in November 1966, 16 consolidation check dams were built in the torrent to reduce bed instability and flooding hazard of the Canal San Bovo village. The check dams have a height of 3.5 m or greater and after their construction they completely blocked the fish run during the breeding season.

The fish ladders form three rings on the right side of the Vanoi torrent that bypass the check dams, thereby allowing the fish run due to the continuous presence of water and the small- to medium-scale step-pool morphology (i.e., a maximum step height of approximately 0.5 m). The fish ladders, which were built using boulders and big cobbles, offer an excellent case study to analyze step-pool kinematics with regard to a geometrical scale that is intermediate between the laboratory scale and that of a natural step-pool system (maximum step height of 2-2.5 m) [*D'Agostino and Lenzi*, 1998].

Within the channel rings (fish ladders), three reaches were selected according to a criterion of morphological homogeneity (the *TA*, *TB*, and *TS* reaches; Figure 1) with the goal of testing different channel slopes typical of step-pool sequences. Three types of field measurements were conducted: (1) topographical surveys to extract the thalweg profiles and cross-sectional geometry in reference cross sections; (2) grain size analysis of the bed surface; and (3) steady state runs by feeding the step-pool reaches with a certain water discharge, taking measurements and surveying the water surface elevation of selected reference cross sections.

Longitudinal profiles of the thalweg and left/right bank were gauged by means of an optical level, whose precision (1 cm) depends mostly on the stadia positioning on the irregular bed topography. The distance between adjacent points in the topographical survey was always less than 0.15 m. Bed slopes (*S*) were then

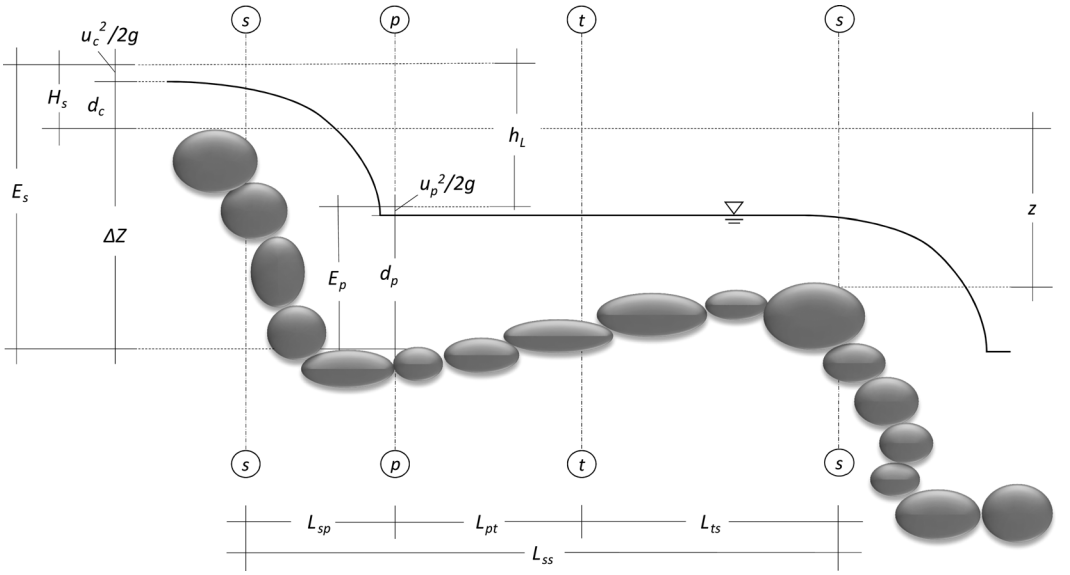

Figure 2. Sketch of the step-pool geometry and energy dissipation [modified from *Wilcox et al*., 2011].

calculated using a linear regression of the bed profiles. A total of 64 cross sections of the type "*s*" (step crest), "*p*" (deepest pool bottom), and "*t*" (intermediate position between pool end and downstream step crest) (Figure 2) were surveyed using a handcrafted tool that consists of a rectangular wooden pole with holes at 3 cm intervals. The wooden pole was fixed on the banks horizontally and placed perpendicular to the main flow direction. A steel rod was inserted vertically into the pole holes until reaching the cross-section contour, thereby obtaining the cross-section topography based on the rod positioning with a precision of 2 mm. The geometric variables (perimeter, wetted area, and flow top width versus water surface elevation) were calculated for the 64 cross sections, and the specific features of the step-pool thalwegs were computed from the detailed profile survey. These characteristics, illustrated in Figure 2, are as follows: the step heights measured from the step crest to the pool bottom (ΔZ), the drop height measured from the two next step crests (z); the horizontal distance between successive steps, L_{ss}; the horizontal distance between the crest of the step and the bottom of the pool, L_{sp}; and the step height-wavelength ratio, $\Delta Z/L_{ss}$.

The grain-size distributions of the bed were obtained by means of a straight-line number-based sampling method. Two sampling stretches were chosen and 200 pebbles (intermediate axis) were measured for each sample using a calliper and adopting a measurement interval of 0.40 m, which is approximately equal to the maximum diameter found in the bed. The relative and cumulative frequency distributions were calculated, and the characteristic diameters (D_{xx}, the diameter at which the *xx* passing diameter by number is finer) were determined.

Artificial flow rates (Q) were generated in the three reaches by regulating the water inflow from the Vanoi torrent at the fish ladder intake. The flow regulation was obtained through a gate for the lowest flow discharges ($0.005\ m^3/s \leq Q \leq 0.043\ m^3/s$) and by using auxiliary pumps for the others ($0.043\ m^3/s < Q \leq 0.234\ m^3/s$), always remaining in the field of a nappe flow regime for *TA* and *TB* reaches and in the region of dominant skimming flow for the *TS* reach. The flow rate measurements were conducted by means of the saline dilution method [*Calkins and Dunne*, 1970], using sodium chloride (NaCl) as tracer. This method is well suited to the turbulent mixing regime in step pools, where a mean absolute error of 8% was obtained by *D'Agostino* [2004]. After injection of the salt-water solution, the electric conductivity was recorded every 5 s. For the same discharge, the flow rate measurement was repeated three times using three different appropriate [*D'Agostino*, 2008] salt quantities, 100, 200, and 300 g, previously dissolved in 20 L of water. These three measurements were averaged to obtain the final value of the run.

During each run and after a positive time check of the steady state regime, the water surface elevations were surveyed in the reference cross sections "*s*", "*p*", and "*t*" using the tool (wooden pole and steel rods) previously described for the channel topography. In the case of turbulent flow, the water surface elevation resulted from

the average of all cross-stream levels of the water surface in the measured section. The hydraulic depths (d) in these cross sections were computed as the ratio between the wetted area (A) and the flow top width (w). The corresponding local mean flow velocities (u; precisely u_s, u_p, u_t) were derived from the continuity equation. For section "*s*" (Figure 2) in *TA* and *TB*, the verification of the critical flow conditions (the unit Froude number) was conducted by measuring the water depth upstream of the step lip and at a distance precisely equal to 3.5 times the depth at the step lip. According to hydraulic considerations [*Chow*, 1973], the depth in this section is equal to the theoretical critical depth—$d_c = (q^2/g)^{1/3}$, where $q = Q/w$—only when the flow regime approaching the step is subcritical. Because agreement between the measured flow depth and theoretical critical depth was good (the maximum absolute difference between the two equaled up to 10%), the local velocity at the *TA-TB* step crest was calculated using the critical-condition formula: $u_c = (g\, d_c)^{1/2}$ and assuming the value of d_c provided by Q and the measured flow width w.

Particular attention was dedicated to quantifying the effective mean travel flow velocity over the whole path of each step-pool reach. This velocity, defined here as the "reach-averaged velocity" (U), was calculated as a combination of the local velocities in sections "*s*", "*p*", and "*t*", considering that U results from the ratio of total length divided by the sum of subreach travel times between the section types: from "*s*" to "*p*" (reach length L_{sp}), from "*p*" to "*t*" (reach length L_{pt}), and from "*t*" to "*s*" (reach length L_{ts}). The flow transfer time between cross sections was considered using the following: (i) the velocity at the step ($u_s = u_c$) over the distance L_{sp}; (ii) the mean of the velocities at the pool center (u_p) and at the section "*t*" (u_t) over the distance $L_{pt;}$ (iii) the mean of u_t and u_c over the distance L_{ts} (Figure 2). Finally, U was obtained as the ratio of the horizontal reach length over total transfer time ("weighted velocity approach"). Finally, a set of empirical formulas reported in the literature to predict mean velocity in steep mountain streams were tested.

The values of the observed U velocities were compared with those predicted by using the relationships listed in Tables 1 and 2. The predictive performance of each equation, regardless of whether it predicts U, U^* or U^{**}, was assessed by means of the root mean square error (*RMS*), quantifying the following standard deviation of the residuals of N data:

$$RMS = \sqrt{\frac{\sum \left(U_{predicted} - U_{observed}\right)^2}{N}} \tag{22}$$

The "at station" measurements also supported the flow energy (E_i) per unit fluid weight determination in each cross section as follows:

$$E_i = Z_i + d_i + \alpha\left(\frac{u_i^2}{2g}\right) \tag{23}$$

where, for the *i-th* cross section, Z_i (m) is the thalweg elevation with respect to a reference datum, d_i (m) is the flow depth, u_i is the "at station" flow velocity (m/s), and α is the kinetic correction factor, which accounts for the velocity distribution within the section (Coriolis coefficient). In a flume experiment, α was observed to vary between 1.05 and 1.08 [*Chen*, 1992], though practically its value does not influence the results [*Wilcox et al*., 2011], and it was set to 1.

The unit energy loss between the two cross sections "*s*" and "*p*" is equal to the difference, h_L (m), in the total flow energy between the upstream and downstream cross sections, and this loss represents the energy dissipation due to the conversion of mechanical energy into heat energy [*Henderson*, 1966; *Roberson and Crowe*, 1997]. In a mountain stream, when studying the reach drop at a step, the energy balance can be written as follows [*Pasternack et al*., 2006; *Wyrick and Pasternack*, 2008]:

$$E_s = H_s + \Delta Z = E_p + h_L \tag{24}$$

where E_s and E_p are the total flow energies in the step and pool cross sections, respectively; H_s (m) is the specific energy at the step (flow depth plus kinetic head); and ΔZ (m) is the step height (Figure 2). The h_L can be converted to a dimensionless form (relative dissipation ΔE_r) by applying the following equation [*Wilcox et al*., 2011]:

$$\Delta E_r = \frac{h_L}{H_s + \Delta Z} \tag{25}$$

Table 3. Main Characteristics of the Step-Pool Sequences of the Experimental Reaches *TA*, *TB*, and *TS*[a]

Reach	*n. sect.*	*n. "s"*	*n. "p"*	*n. "t"*	Z_t (m)	*L* (m)	*S* (m/m)	σ_z (m)
TA	22	8	7	7	2.08	35.39	0.060	0.244
TB	19	7	6	6	2.14	19.99	0.100	0.279
TS	23	8	8	7	1.06	42.98	0.026	0.078
TOTAL	64	23	21	20				

[a]*n. sect*. is number of cross sections within the reach; *n. "s"* is number of section "*s*" (steps); *n. "p"* is number of pools; *n. "t"* is number of sections "*t*" (pool exit); Z_t is difference in height between the first and last cross section of the reach; *L* is the planimetric length of the reach; *S* is the mean reach slope; and σ_z is standard deviation of the elevations with respect to the line fitting the longitudinal profile.

In this research, the energy analysis was performed for the *TA* and *TB* reaches focusing on the spill resistance assessment in morphologically distinct step-pools. The calibration of an empirical relationship was performed to predict the energy dissipations, ΔE_r, assessed in the field experiments.

3. Results

3.1. Reach Topography and Bed Grain-Size Distributions

The 64 cross sections ("*s*", "*p*", "*t*") of *TA*, *TB*, and *TS* reaches feature mean channel widths of 0.2–2.0 m within the measured discharge field and belong to typical thalweg gradients of step-pool systems: 6.0%, 10.0%, and 2.6%, respectively. In terms of morphology, the *TA* and *TB* reaches fall fully in the step-pool type (Figures 1a and 1b), whereas *TS* belongs to the stepped transitional type between plane-bed and step-pool category (Figure 1c). The step-pool reaches cover a range of step height, measured from the crest to the bottom of the downstream pool, from 0.03 to 0.84 m. The step spacing, L_{ss}, ranges from 2.94 to 8.98 m (Table 4). A total of 22 cross sections were surveyed in reach *TA*, 19 in reach *TB*, and 23 in reach *TS* (23 steps, 21 pools, and 20 pool exits). The main geometric characteristics are listed in Tables 3 and 4.

For the bed surface roughness, Table 5 summarizes the results of the pebble count analysis of the sampled bed areas. The mean diameter (D_{mean}) was found to be 0.084 m for the combined reach *TA-TB*, whereas a slightly finer value of 0.064 m was obtained for the *TS* reach. Both samples have a heterogeneous composition of fine gravel to boulders and an asymmetric distribution shifted toward the coarse component. The two grain-size curves are characterized by the closeness of their D_{16} and D_{50} diameters (Table 5), and by the difference of their D_{90} values, which are equal to 0.41 m for *TA-TB* and 0.22 m for *TS*.

Table 4. Geometrical "Step-to-Pool" Features of the Three Experimental Reaches (*n.* step is the step numbering)

Reach	*n. step*	ΔZ (m)	L_{ss} (m)	L_{sp} (m)	*z* (m)
TA Step pool	1	0.60	4.61	1.08	0.22
	2	0.60	4.56	1.11	0.16
	3	0.49	3.90	1.38	0.35
	4	0.47	4.64	0.69	0.44
	5	0.47	4.62	1.09	0.19
	6	0.61	5.85	1.24	0.23
	7	0.71	7.20	1.02	0.48
	Mean	0.56	5.06	1.09	0.30
TB Step pool	1	0.73	3.05	0.70	0.38
	2	0.64	3.91	1.03	0.44
	3	0.52	3.64	1.53	0.20
	4	0.69	2.95	0.95	0.26
	5	0.84	3.50	1.16	0.43
	6	0.61	2.94	1.05	0.44
	Mean	0.67	3.33	1.07	0.36
TS Transitional between step-pool and plane-bed	1	n.d.[a]	6.07	0.41	0.12
	2	n.d.	4.71	0.51	0.18
	3	n.d.	4.54	0.54	0.23
	4	n.d.	5.94	0.56	0.17
	5	n.d.	7.48	0.59	0.10
	6	n.d.	4.83	0.46	0.16
	7	n.d.	8.98	0.66	0.09
	8	n.d.	-	0.44	0.00
	Mean	-	6.08	0.52	0.15
Mean		-	4.82	0.89	0.27
Standard Deviation		-	1.61	0.33	0.13
Maximum		-	8.98	1.53	0.48
Minimum		-	2.94	0.41	0.09

[a]n.d. = not detectable.

3.2. Flow Velocities and Apparent Manning's *n* Coefficient

The calculated values of the steady discharges, which are associated with each run in the three fish ladder (*TA*, *TB*, and *TS*) reaches, are listed in Table 6. The minimum and maximum unit discharges fall within the range $q = 0.004$–0.215 m^2/s. A total number of 290 velocities were back calculated in sections "*s*", "*t*", and "*p*". The *u* values range from a minimum of 0.008 m/s in a "*t*" type section to a maximum of 3.17 m/s in a step section "*s*" (*TS* reach). The highest values in section "*s*" could be due to errors caused by the

Table 5. Main Characteristic Diameters and Basic Statistical Descriptors of the Pebble Count Analysis

Reach	*TA - TB*	*TS*	Reach	*TA - TB*	*TS*
	D_{xx} (mm)		Uniformity coefficient	9.59	3.61
D_{10}	14	23	Gradation coefficient	3.18	2.47
D_{16}	26	29	Standard deviation	3.15	2.47
D_{50}	95	71	Asymmetry coefficient	0.39	0.27
D_{60}	135	83			
D_{70}	170	110			
D_{84}	260	176			
D_{90}	406	219			
D_{mean}	84	64			

difficulty of measuring the flow width in narrow conditions. The average values and standard deviation are 1.57 ± 1.55 m/s in section "*s*", 0.31 ± 0.59 m/s in section "*p*", and 0.31 ± 0.52 m/s in section "*t*". The range of Froude numbers accounting for "*t*" and "*p*" cross sections varies from 0.008 to 0.427. Based on these data, the reach-averaged *U* velocities were obtained, as well as the average "at station type" *u*′ flow velocities within each reach (mean *u* values for *TA* or *TB* or *TS* in the section type "*s*" or "*p*" or "*t*": u'_s, u'_p, u'_t; Figure 3). The *U* values were also grouped for *TA*, *TB*, and *TS* reaches, highlighting the inverse role of step height (Table 4) and channel gradient (Table 3) on the *U* values (Figure 4). In fact, the results show that when *Q* is constant, the larger the reach gradient/step height/standard deviation of bed elevation is, the lower the *U* is (Figure 4). Table 6 also lists the values of Manning's *n* coefficient for each run. These were calculated by approximating the mean hydraulic radius of each run as the average (d_m) of the three hydraulic depths in "*s*", "*p*", and "*t*" sections, and assuming the reach slope *S* (Table 3) is equal to the energy gradient. With this information, Manning's *n* coefficient can be termed "apparent" because the energy slope used in the normal depth equation is fictitious.

The prediction results in terms of reach-averaged velocities *U* after the application of the formulas listed in Tables 1 and 2 are plotted in Figure 5 together with the related *RMS* error, which was computed separately for each reach (*TA, TB*, and *TS*) as well as for the whole sample.

3.3. Energy Dissipation Due to the Drop

The energy analysis, as stated in the methodology section, was carried out for the *TA* and *TB* reaches, which have more evident step-pool morphology and steeper slopes. Following the calculations of the dissipations (h_L) for each step-pool sequence and unit discharge *q*, their dimensionless values (ΔE_r, equation (25)) were calculated. The results on the ΔE_r are listed in Tables 7 and 8 for the *TA* and *TB* reaches, respectively. The measured values vary from 0.46 to 0.75 in the *TA* reach and from 0.33 to 0.71 in the *TB* reach. As found by *Rajaratnam and Chamani* [1995; Figure 7 on page 380] in their investigations on the energy loss at drops, ΔE_r should be described through a power function that contains, as an independent variable, the ratio between the critical depth and the drop height or, because the critical depth is strictly related to the pool water depth, the ratio of the pool depth to drop/step height [*Rajaratnam and Chamani*, 1995; Figure 8 on page 381].

Table 6. Average "At Station Type" *u*′ Flow Velocity (the Subscript "*s*" or "*p*" or "*t*" Indicates the Section Type), Reach-Averaged Flow Velocity *U*, and Manning's *n* Coefficient for the Three Study Reaches (*d* = Depth; *w* = Top Width of the Flow)

	Q	*U*	w_s	w_p	w_t	d'_s	d'_p	d'_t	u'_s	u'_p	u'_t	*n*
Run	(m^3/s)	(m/s)	(m)	(m)	(m)	(m)	(m)	(m)	(m/s)	(m/s)	(m/s)	(-)
TA-1	0.005	0.08	0.27	1.29	0.96	0.04	0.22	0.21	0.93	0.03	0.03	0.92
TA-2	0.031	0.29	0.37	1.52	1.09	0.10	0.25	0.25	1.76	0.12	0.09	0.29
TA-3	0.043	0.35	0.44	1.57	1.13	0.11	0.26	0.26	1.85	0.16	0.12	0.25
TA-4	0.118	0.56	0.74	1.76	1.31	0.15	0.31	0.32	1.68	0.31	0.23	0.18
TA-5	0.178	0.63	1.07	1.89	1.47	0.15	0.33	0.35	1.39	0.38	0.29	0.17
TB-1	0.005	0.05	0.40	1.35	1.15	0.03	0.34	0.29	0.25	0.01	0.02	2.40
TB-2	0.031	0.19	0.52	1.49	1.28	0.09	0.37	0.33	0.94	0.07	0.07	0.70
TB-3	0.043	0.20	0.82	1.64	1.34	0.08	0.40	0.34	0.68	0.08	0.08	0.65
TB-4	0.114	0.36	1.09	1.95	1.47	0.14	0.46	0.40	1.31	0.17	0.16	0.43
TB-5	0.189	0.51	1.20	2.03	1.61	0.16	0.46	0.43	1.30	0.26	0.23	0.31
TS-1	0.013	0.27	0.24	0.74	0.80	0.71	0.14	0.09	0.74	0.13	0.24	0.14
TS-2	0.041	0.50	0.39	0.92	0.85	0.26	0.18	0.14	0.98	0.30	0.35	0.10
TS-3	0.074	0.55	0.67	1.10	1.00	0.12	0.28	0.22	1.19	0.30	0.37	0.11
TS-4	0.234	0.80	1.17	1.38	1.09	0.17	0.32	0.29	1.35	0.75	0.69	0.08

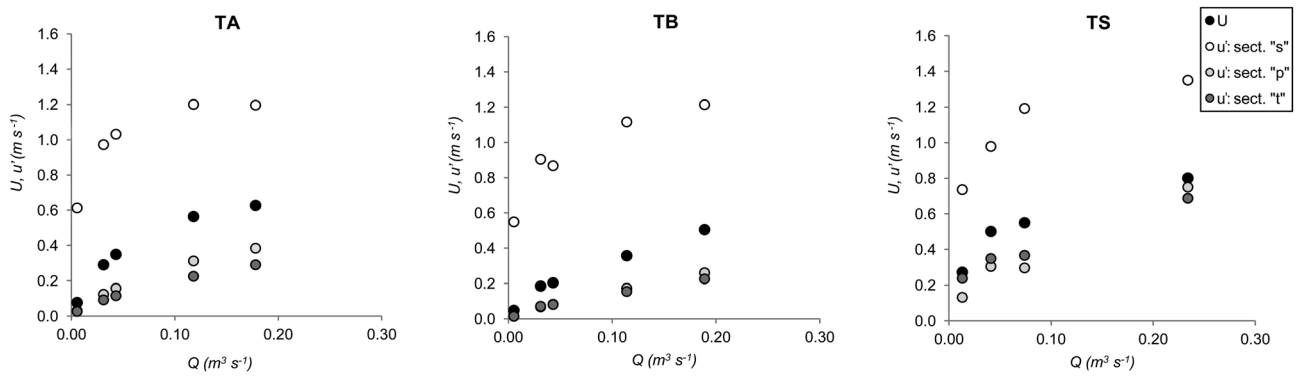

Figure 3. At station ("s", "p", "t") mean flow velocities *u'* and reach-averaged mean flow velocities *U* versus the flow rate of each experimental run: *TA* reach, *TB* reach, and *TS* reach.

In our case of a series of irregular step-pool drops, the latter ratio ($d_p/\Delta Z$) is more effectively related to ΔE_r (adjusted *R-squared* = 0.74; *residual standard error* = 0.06) and is more significant than the $d_c/\Delta Z$ ratio (adjusted *R-squared* = 0.22; *residual standard error* = 0.10) and the D_{50}/d_c relative roughness (adjusted *R-squared* = 0.01; *residual standard error* = 0.11), which *Pagliara and Chiavaccini* [2006] also found to be lowly correlated to ΔE_r for a ramp. Thus, the following empirical fitting equation has been obtained (Figure 6):

$$\Delta E_r = 0.38\left(\frac{d_P}{\Delta Z}\right)^{-0.59} \tag{26}$$

Equation (26) highlights a clear decreasing trend of relative dissipation ΔE_r from 75% to 40% when the relative pool depth $d_p/\Delta Z$ increases from 0.30 to 0.85. Table 9 summarizes the main statistics and the analysis of variance of the fitted model, equation (26), which explains most of the variability of the ΔE_r field observations.

4. Discussion

Knowledge of the step-pool kinematics in natural streams should be verified under the widest range of morphological and hydraulic conditions. The results obtained from the experiment fall within a range of conditions that are poorly explored in the literature. In fact, they represent an intermediate situation between small-scale laboratory data (maximum ΔZ values and flow widths equal to 0.84 and 2.0 m, respectively) and field data from step pools with step heights equal to 0.5–2 times the medium boulder size. For the hydraulic conditions (Figure 2), according to the regions defined by the dimensionless upstream step head, $(H_s+\Delta Z)/H_s$ versus dimensionless submergence, $(E_s\text{-}E_p)/H_s$ [*Wyrick and Pasternack*, 2008, p. 10], the experimental runs in the *TA* and *TB* reaches fall in the region of pushed-off jumps (jumps downstream from the base of the impacting nappe) and classic hydraulic jumps with some points (highest *Q*) at the boundary of the drowned jump regime. The *TS* reach falls mostly in the category with a dimensionless step head lower than 2 ($\Delta Z < H_s$), and its behavior is basically that of no jumps with a few local drowned jumps.

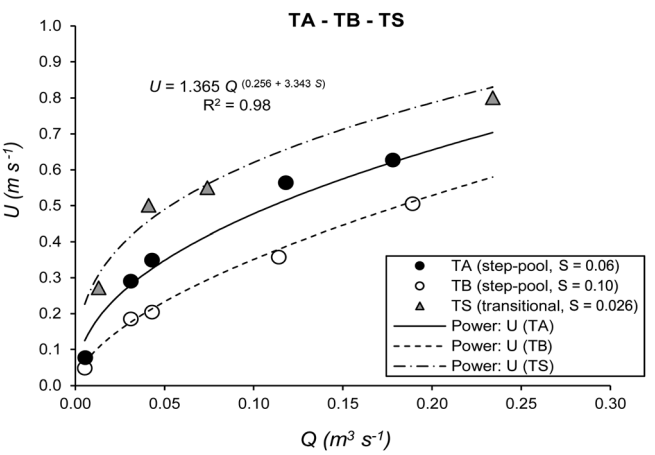

Figure 4. Overall calibration of the power function trends of reach-averaged mean flow velocities *U* versus the flow rate *Q* in the three reach types (*TA*, *TB*, and *TS*).

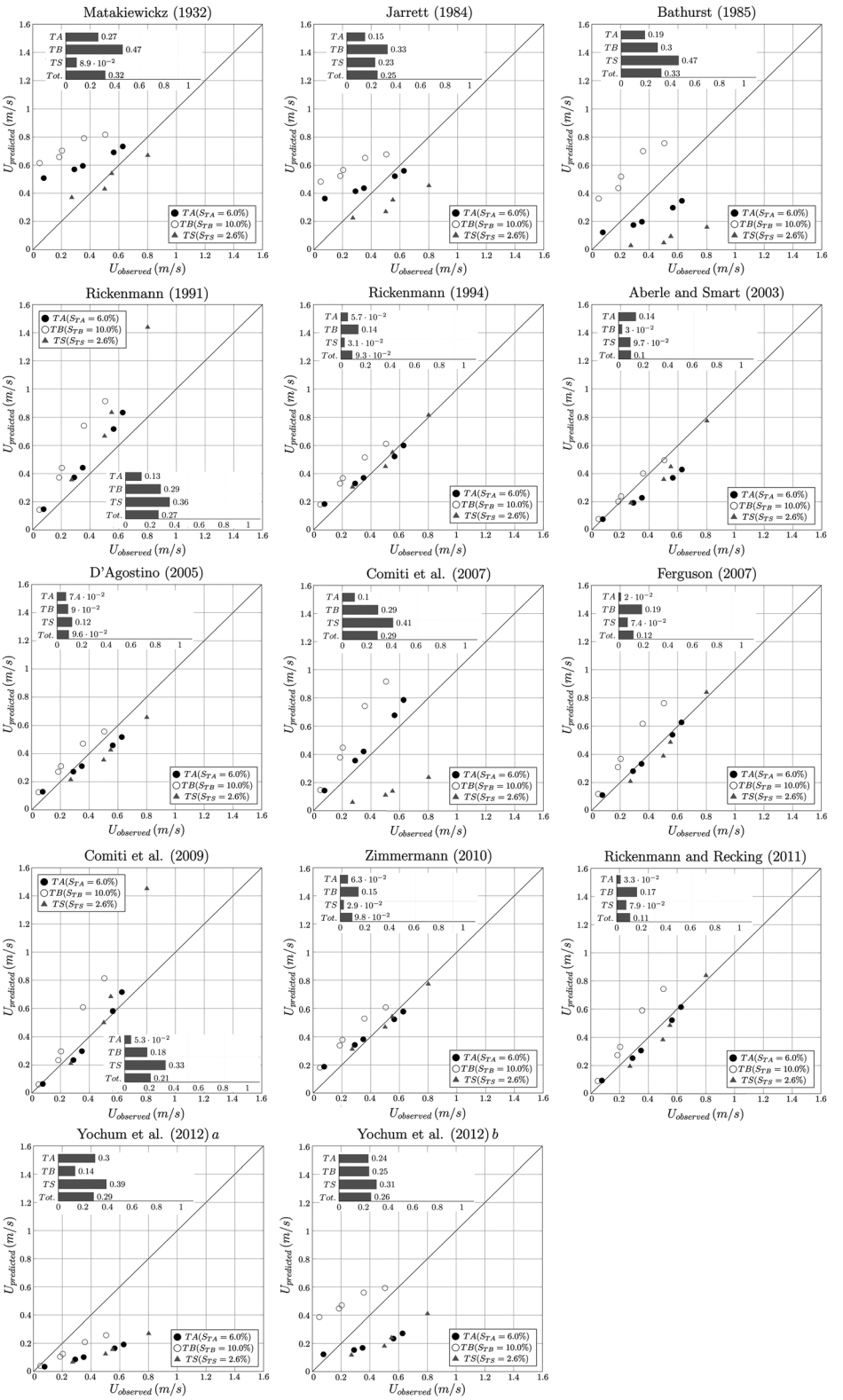

Figure 5. Plot of experimental *U* values versus those predicted using formulas of Tables 1 and 2 and indicated in each comparative graph. The root mean square (*RMS*) errors (partial and total, "*Tot*") are also reported in each graph.

Table 7. Field Data: Variables for the ΔE_r Calculations for the *TA* Reach (ΔZ Values Are Listed in Table 3; *n.* Step Is the Step Numbering)

n. step	q (m^2/s)	H_s (m)	E_s (m)	d_p (m)	u_p (m/s)	h_L (m)	ΔE_r (-)
1	0.02	0.05	0.64	0.207	0.03	0.44	0.68
2	0.01	0.04	0.64	0.263	0.02	0.38	0.59
3	0.01	0.04	0.52	0.226	0.02	0.30	0.57
4	0.04	0.08	0.55	0.153	0.05	0.40	0.72
5	0.04	0.08	0.54	0.249	0.02	0.30	0.54
6	0.02	0.05	0.66	0.221	0.03	0.43	0.66
7	0.04	0.08	0.79	0.200	0.04	0.59	0.75
1	0.08	0.13	0.73	0.259	0.11	0.47	0.64
2	0.07	0.12	0.72	0.266	0.09	0.45	0.63
3	0.04	0.09	0.57	0.263	0.09	0.31	0.54
4	0.17	0.21	0.68	0.213	0.19	0.47	0.68
5	0.08	0.13	0.60	0.239	0.10	0.36	0.60
6	0.10	0.15	0.75	0.246	0.11	0.51	0.67
7	0.18	0.22	0.93	0.239	0.18	0.69	0.74
1	0.09	0.14	0.74	0.286	0.14	0.45	0.61
2	0.09	0.15	0.75	0.268	0.13	0.48	0.64
3	0.06	0.11	0.60	0.278	0.11	0.32	0.53
4	0.21	0.25	0.72	0.232	0.24	0.48	0.67
5	0.07	0.12	0.58	0.257	0.12	0.33	0.56
6	0.12	0.17	0.78	0.251	0.15	0.53	0.68
7	0.22	0.26	0.97	0.259	0.22	0.71	0.73
1	0.11	0.16	0.76	0.355	0.27	0.40	0.53
2	0.22	0.25	0.86	0.310	0.28	0.54	0.63
3	0.16	0.21	0.70	0.360	0.21	0.33	0.48
4	0.16	0.21	0.68	0.246	0.42	0.42	0.62
5	0.12	0.17	0.63	0.328	0.25	0.30	0.48
6	0.12	0.17	0.78	0.269	0.29	0.51	0.64
7	0.40	0.38	1.09	0.295	0.46	0.78	0.72
1	0.12	0.17	0.77	0.401	0.33	0.36	0.47
2	0.12	0.17	0.78	0.325	0.35	0.45	0.57
3	0.20	0.24	0.73	0.415	0.28	0.31	0.42
4	0.15	0.20	0.67	0.211	0.46	0.45	0.67
5	0.16	0.20	0.67	0.356	0.34	0.31	0.46
6	0.18	0.22	0.83	0.314	0.37	0.51	0.61
7	0.19	0.23	0.94	0.319	0.55	0.60	0.64

The results of the kinematics behavior suggest that the majority of the spatial u variation occurs from the step head zone to the pool area and between the intermediate section (pool exit zone; section "*t*" in Figure 2) and the successive step. By contrast, the subreach pool center-pool exit maintains practically the same mean velocity, and the small variations depend mainly on the local narrowing or widening of the channel. In all reaches, the u values generally increase with the water discharge but in the sections "*p*" and "*t*" based on an almost linear function, while in section "*s*" based on a power law function (Figure 3). For the highest Q, a flat trend of u' emerges in the section "*s*" and this is caused by the cross-section widening and then by the q invariance even if Q rises. The comparison of the spatially reach-averaged velocity U and the "at station type" u' values suggests that the larger weight of u' in pools and pool ends is evident in the U value determination. The latter ranges between 2.2 and 3.2 times the u' velocity in the "*t*" section (u'_t) for the *TA* and *TB* step pools and between 1.1 and 1.5 times u'_t in the *TS* transitional reach. In contrast, the ratio between U and the u' velocity at the step head (u'_s) is highly variable and reaches its maximum variation in step-pool reaches (U/u'_s values from 1/11.4 to 1/1.9 in *TA-TB* versus ratios of 1/2.7 to 1/1.7 in the *TS* reach). For the same reason, the overall calibration of a power function trends of U versus Q and S variables ($U = k\,Q^{(j\,+\,m\,S)}$, adjusted *R-squared* = 97.98%; k, j, and m are the calibration parameters reported in Figure 4) provides the highest values of the exponent of Q for *TA* and *TB* (0.46 and 0.59, respectively) and a much lower value for the *TS* reach (0.34). This finding is in agreement with previous observations, which emphasized how the energy-line slopes of rough morphologies change more rapidly when a macroroughness regime shifts to a microroughness or to a transition-to-microroughness regime [*Bathurst*, 1985; *Smart*, 1999; *Dingman*, 2007].

The comparison of the lower Q-U curves for *TA* and *TB* with the *TS* curve (Figure 4) extends the flow regime theory at the scale of a step-pool sequence and highlights the key role of the spill resistance in well-defined step-pool units. Here, the majority of the total energy dissipation in step-pool reaches depends on the series of spill resistances and, according to equation (26), on the relative submergence with regard to the step height ($d_p/\Delta Z$). Indeed, the insertion of equation (26) into equation (24) allows this latter to be solved for d_p and u_p, which also, given Q, is a function of the unique unknown d_p. Spill resistance due to the drop and according to equation (26) (Figure 6) is capable of consuming up to 75% of the available energy at the step when the water depth at the pool center (d_p) is equal to 30% of the step height. As the d_p increases to 85% of ΔZ, the spill dissipation reaches an experimental minimum of approximately 40% of the available energy, which is remarkable given the short distance between the step crest and pool center.

Table 8. Field Data: Variables for the ΔE_r Calculations for the *TB* Reach (ΔZ Values Are Listed in Table 3; *n*. Step Is the Step Numbering)

n. step	q (m^2/s)	H_s (m)	E_s (m)	d_p (m)	u_p (m/s)	h_L (m)	ΔE_r (-)
1	0.01	0.03	0.76	0.411	0.01	0.35	0.46
2	0.00	0.02	0.67	0.376	0.01	0.29	0.44
3	0.06	0.11	0.62	0.364	0.02	0.26	0.41
4	0.03	0.06	0.75	0.309	0.01	0.44	0.59
5	0.01	0.04	0.87	0.255	0.02	0.62	0.71
6	0.02	0.06	0.67	0.323	0.01	0.35	0.52
1	0.04	0.08	0.81	0.408	0.05	0.41	0.50
2	0.02	0.05	0.70	0.415	0.05	0.29	0.41
3	0.30	0.31	0.83	0.411	0.08	0.42	0.50
4	0.13	0.18	0.87	0.368	0.06	0.50	0.58
5	0.04	0.09	0.92	0.275	0.09	0.64	0.70
6	0.08	0.13	0.74	0.358	0.06	0.39	0.52
1	0.03	0.07	0.80	0.458	0.06	0.34	0.43
2	0.02	0.05	0.70	0.420	0.07	0.28	0.40
3	0.21	0.25	0.77	0.420	0.10	0.35	0.45
4	0.15	0.19	0.89	0.397	0.08	0.49	0.55
5	0.06	0.10	0.94	0.304	0.10	0.64	0.68
6	0.06	0.10	0.72	0.372	0.09	0.34	0.48
1	0.06	0.10	0.84	0.561	0.13	0.28	0.33
2	0.04	0.09	0.73	0.444	0.15	0.29	0.39
3	0.51	0.45	0.96	0.409	0.20	0.55	0.57
4	0.38	0.37	1.06	0.461	0.17	0.60	0.56
5	0.08	0.13	0.96	0.378	0.21	0.58	0.61
6	0.10	0.15	0.76	0.502	0.16	0.26	0.34
1	0.09	0.14	0.87	0.541	0.21	0.33	0.38
2	0.07	0.12	0.77	0.447	0.25	0.32	0.41
3	0.30	0.31	0.83	0.387	0.30	0.44	0.53
4	0.58	0.49	1.18	0.462	0.25	0.71	0.61
5	0.12	0.17	1.00	0.406	0.31	0.59	0.59
6	0.16	0.21	0.82	0.518	0.24	0.30	0.36

Similarly, in Italy's Rio Cordon step pools (reach slopes of 0.10–0.13 m/m), *Wilcox et al*. [2011] found a relative head loss, ΔE_r, in the range of 0.37–0.78 and concluded that the energy dissipation is approximately two-thirds of the total energy. The dissipative function—equation (26)—depicts a more precise trend of such dissipation (Figure 6), which can be verified by using the Rio Cordon data. This allows the investigation of how equation (26) responds to natural step-pool data under greater flow rates ($Q = 0.8$–1.3 m^3/s) and larger step-pool sizes ($\Delta Z = 0.3$–1.6 m; step width = 3.3–6.6 m). The results of the application of equation (26) to *Wilcox et al*. [2011] data (Figure 7) are consistent and demonstrate its promising robustness. In fact, the Vanoi torrent data set provides a *RMS* (equation (22) with variable ΔE_r instead of *U*) equal to 0.096, which remains satisfactory upon adding the Rio Cordon data (*RMS* = 0.114) or simply analyzing the *Wilcox et al*. [2011] data separately (*RMS* = 0.194). More investigations to refine the uncertainties of equation (26) should focus on the conditions of maximum energy dissipation, where the experimental data appear to be slightly overestimated, and where an experimental upper limit of the energy dissipation is approximately 80%. Less problematic is the spreading of data with medium/low dissipations, where the points are more symmetrically distributed around the line of perfect agreement, and where the biases (particularly for the lowest ΔE_r) could depend on the local step-lip morphology, which is capable of influencing the nappe immersion when d_p is close to ΔZ. The same importance of the step and pool configuration was highlighted by *Zimmermann and Church* [2001], who concluded that energy dissipated in the pool depends on the height and configuration of the upstream step. The specific 3-D topography of each step-pool pair could also generate the biases, although *Yochum et al*. [2014] showed that flow resistance prediction using relative bedform submergence computed from the three-dimensional variability provides no decisive advantages with respect to submergence computed from simpler-to-measure longitudinal profiles.

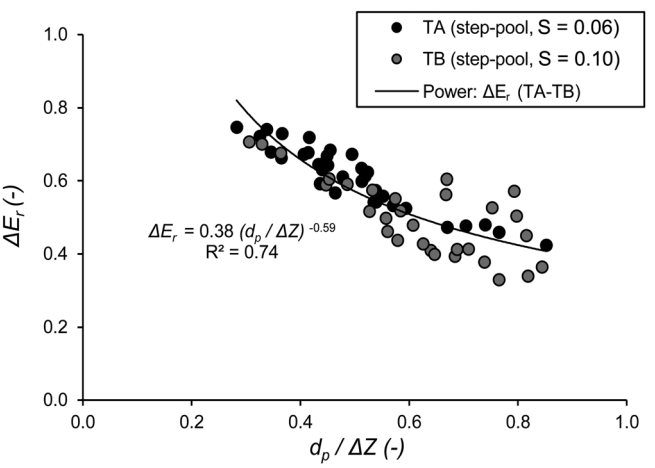

Figure 6. Relative energy dissipation ΔE_r versus relative pool depth ($d_p/\Delta Z$): field data and fitting model.

Further analysis of the results in Tables 7 and 8 proves that the relative pool depth ($d_p/\Delta Z$) and the amount of flowing mass become the driving factors of energy dissipation, even despite the overall bed gradient. In fact, based also

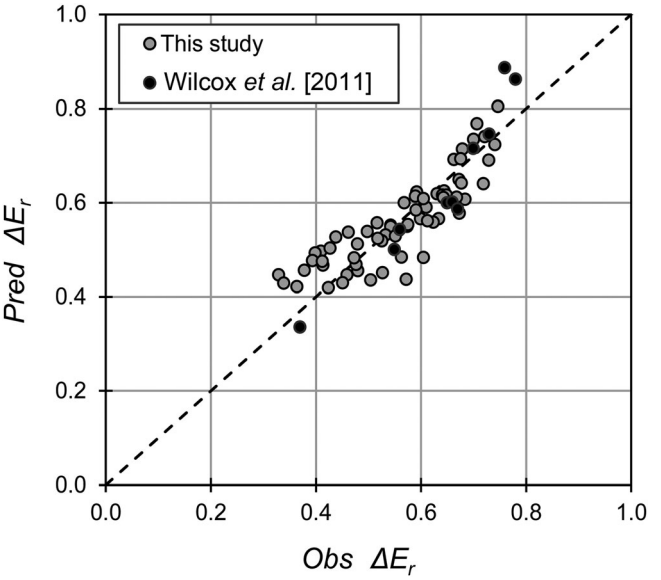

Figure 7. Observed (*Obs*) dimensionless energy dissipation ΔE_r versus the corresponding predicted (*Pred*) values through equation (26): *TA* and *TB* reaches.

on Figure 4, the same water discharge produces *U* trends that are progressively shifted to higher *U* values as the slope decreases, which corresponds topographically to lower relative drop heights. *Pagliara and Chiavaccini* [2006] suggested that the relative energy dissipation through a ramp can be reduced to a function of two parameters, the relative submergence and slope, the slope being inversely related to the energy dissipation. In our experiments, step-pool reach *TB*, the steepest, shows *U* values lower than those of step-pool reach *TA*, which in turn registers *U* values lower than those of the transitional reach *TS*. Hence, both a decreasing relative submergence and an increasing reach slope seem to cooperate in promoting an increment in energy dissipation. Such behavior is also visible in the back-calculation of Manning's *n* coefficient of the turbulent flow resistance equation (Table 6) and subsequent data plotting (Figure 8). Here, the d_m/σ_z variable, similar to that considered by *Aberle and Smart* [2003], *Yochum et al.* [2012] and *Yochum et al.* [2014], was scaled to the reach slope *S* obtaining a collapse of all the experimental data in the following semilogarithmic law (Figure 8):

$$n = \frac{1}{\left[3.68\ ln\left(\frac{d_m}{\sigma_z\ S}\right) - 6.47\right]} \tag{27}$$

Equation (27) has an adjusted *R-squared* = 92.88% and, based on the ANOVA analysis (Table 10), it properly assesses the flow resistance over a fairly wide range of experimental discharges (from 0.005 to 0.234 m^3/s) and relative d_m/σ_z submergences (from 0.64 to 3.30). The adjusted *R-squared* of the semilogarithmic law that results from considering d_m/σ_z, instead of $d_m/(\sigma_z, S)$ would be reduced to 80.11% ($1/n = 3.44 + 6.96\ ln\ d_m/\sigma_z$) due to the data-point separations between the *TA* and the *TB* reach, having d_m/σ_z values of 0.64–1.13, and 0.79–1.26, respectively. The last occurrence is a confirmation of the findings of *David et al.* [2010], who highlighted the way in which the prediction of the flow resistance is greatly improved in step pools when the variable of relative step submergence (hydraulic radius *Rh* divided by ΔZ) is considered in addition to the bed slope. The same authors found that holding the bed slope constant produces no significant differences in the friction factor between the transitional reach (plane-bed/step-pool) and step-pool channels. Our result does not contradict this statement because there is no overlap in the Vanoi torrent experiments between the slope of the transitional reach *TS* (2.6%) and the slopes of the *TA-TB* step-pool reaches (6% and 10%, respectively). In our case, the *TS* reach achieves higher *U* values because the overall submergence of the bed irregularities is

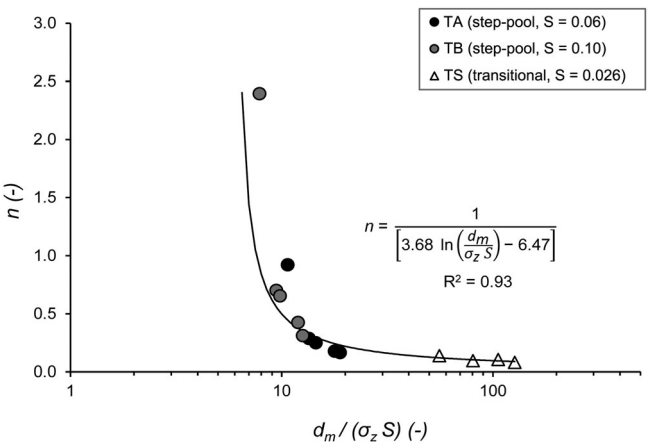

Figure 8. Overall trend of the experimental data: ratio of the relative submergence and the averaged reach slope ($d_m/\sigma_z\ S$) versus Manning's *n* coefficient.

Table 9. Parameters, Statistical Indices, and Results of the Analysis of Variance of the Fitted Model of Equation (26)

Coefficients					Analysis of Variance		
Parameters	Estimated Values	Asymptotic Standard Error	Asymptotic 95% Confidence			Sum of Squares	Mean Square
Coefficient	0.381	0.013	0.355	0.407	Model	20.977	10.489
Exponent	−0.591	0.044	−0.679	−0.504	Residual	0.196	0.003
					Total	21.173	
R-squared (%)			74.481				
R-squared adjusted (%)			74.076				
Standard Error of Estimation			0.056				
Mean absolute error			0.044				

greater than 1.3 times the standard deviation of the longitudinal bed profile (σ_z). Below such a drowning threshold—approximately $d_m/\sigma_z = 1.3–1.5$; $d_m/(\sigma_z\, S) = 15–20$ (Figure 8)—the resistance develops and rises rapidly through the dominant spill component. Above the threshold, the resistance decreases slowly passing to the grain resistance, the step structures abandon their exclusive control on the dissipation, as stated by *Zimmermann and Church* [2001], the grain resistance becomes dominant over the spill resistance, and Manning's n remains almost constant ($n = 0.1$; Figure 8). Moreover, in *TA-TB* reaches the values of σ_z are close to D_{84} (Tables 3 and 5) and it is worth noting how the relative-submergence threshold of 1.3 agrees with the value indicated by *Bathurst et al.* [1981] to separate macroroughness regime from the transition to micro-roughness regime.

In conclusion, Figure 8 underlines how Manning's equation could still be of some practical use under the following conditions: (i) the assumption of a simplified space-averaged value of the depth (d_m) instead of a specific hydraulic radius (Rh); and (ii) the acceptance of a calibration of Manning's n coefficient as a function of d_m/σ_z or better of $d_m/(\sigma_z\, S)$ regardless of the morphology of a step pool or of a transitional reach between plane-bed and step-pool.

The performance of the tested equations for the U prediction (Figure 5) is additional confirmation of the spill resistance role because almost all formulas emphasizing the weight of the step height (or surrogate variables) and of the flowing mass yield better results. In detail, among the three oldest equations (8), (9), and (10), that of *Bathurst* [1985] (linked to the normal depth equation) does not properly fit the step-pool kinematics ($RMS = 0.330$), the *Jarrett* [1984] formula appears more consistent ($RMS = 0.250$), and the *Matakiewickz* [1932, in *Indri*, 1942] equation is very accurate only for the transitional reach *TS* between plane-bed and step-pool (Figure 5). These earlier formulas were not specifically developed for step-pool channels. The poor agreement observed between the data and these formulas should justify the development of specific formulas for these channel morphologies. Examining the classical power-law relationships to directly compute U, the *Rickenmann* [1994] and *D'Agostino* [2005] equations provide predictions with the best performances (i.e., lowest $RMS = 0.093$ and 0.096, respectively), but the *Aberle and Smart* [2003] formula also features a very high accuracy ($RMS = 0.100$; Figure 5). The single independent variable and high performance of the *D'Agostino* [2005] formula could suggest that, when dealing with steep high-roughness rivers ($d_p/\Delta Z$ dominated), flowing mass per unit width could be capable on its own of robustly predicting U.

Table 10. Parameters, Statistical Indices, and Results of the *ANOVA* Analysis of the Fitted Model of Equation (27)

Coefficient					Analysis of Variance				
			T						
Parameters	Least Squares Estimated	Standard Error	Statistic	p-Value		Sum of Squares	Mean Square	F Ratio	p-Value
Intercept	−6.459	0.944	−6.853	0.0000	Model	165.358	165.358	156.57	0.0000
Slope	3.681	0.294	12.513	0.0000	Residual	12.673	1.056		
					Total	178.032			
R-squared (%)			92.882						
R-squared adjusted (%)			92.288						
Standard Error of Estimation			1.028						
Mean absolute error			0.823						

Considering the equations based on the *U** group, the equation of *Zimmermann* [2010] generates—together with the *Rickenmann* [1994] and *Aberle and Smart* [2003] formulas—one of best *RMS* (0.098). A comparably excellent *RMS* value (0.120) results from the relationship found by *Ferguson* [2007], which has a general tendency to overestimate *U* for the steeper step-pool reach *TB* (Figure 5), similarly to what was previously observed by *Yochum et al*. [2012] and *Lee and Ferguson* [2002] for the same formula. Analyzing the dimensionless *U*** group of equations, the lowest *RMS* (0.110) is given by the *Rickenmann and Recking* [2011] formula with a *RMS* almost equal to that of *Zimmermann* [2010]. Equation (20), proposed by *Yochum et al*. [2012] (*a* in Figure 5), exhibits a general tendency to underestimate the flow velocity *U* particularly for the two lowest slopes (*TA* and *TS*). The large amount of wood present in the reaches studied by *Yochum et al*. [2012] and the nonnaturalness of the sequences of this study (artificial and regularly spaced man-made steps), with low winding of the thalweg and riverbanks, could motivate the different velocity prediction of equation (20), similarly to what was previously stated by *David et al*. [2010, 2011]. In fact, wood presence and expansions and contractions of the channel banks can provide an important additional source of resistance [*Bathurst*, 1985; *Dust and Wohl*, 2012; *Kean and Smith*, 2006]. The *Comiti et al*. [2007] equation, which employs a step-pool-specific steepness factor, produces a certain dispersion of data around the line of perfect agreement, abundantly underpredicting *U* in the gentlest *TS* reach and overpredicting *U* in the steepest *TB* reach. When the three reach types are analyzed separately, the *Ferguson* [2007] equation provides the lowest *RMS* (0.020) and the best fit for the *TA* reach. The *Rickenmann and Recking* [2011], *Comiti et al*. [2009], and *Comiti et al*. [2007] relationships also yield very accurate predictions for *TA*. For the steepest reach, *TB*, the *Yochum et al*. [2012] (equation (20); *a* in Figure 5) and *Zimmermann* [2010] formulas predict—after the formulas of *Aberle and Smart* [2003] and *D'Agostino* [2005]—the most correct values. The *Yochum et al*. [2012] formula, based on the relative submergence d_m/σ_z (equation (21); *b* in Figure 5), provides similar *RMS* values for the three reaches and differentiates the behavior of the two step-pool reaches excessively. The *Comiti et al*. [2009] relationship would provide a robust prediction if the *TS* reach, which is morphologically at the boundary of the step-pool morphology, was not considered. The numerous formulas resulting in good/optimum agreement and converging with our field experiments suggest that the method used to assess *U* through the sum of travel times between reference cross sections rather than by means of tracers should not have conditioned the results and, indeed, could support future research focused on the effects of local dissipations (e.g., wood, big boulders, particular pool features) at the scale of single morphological units.

To summarize, the equations that best predict the overall field of the Vanoi torrent experiments and reach a comparable performance are those of *Rickenmann* [1994], *Aberle and Smart* [2003], *D'Agostino* [2005] and *Zimmermann* [2010], and the most precise equations for the step pools (the lowest *RMS* error sums for the *TA* and *TB* reaches) are the formulas of *Aberle and Smart* [2003] and *D'Agostino* [2005], closely followed by those of *Ferguson* [2007] and *Rickenmann and Recking* [2011]. The efforts made by these researchers suggest that rather than proposing new predictive equations of *U* for step-pool systems, the verification of these equations should be performed under different flow rates, geometrical step height sizes, pool lengths, channel widths, and sediment sizes and arrangements. The strength of a simple formula accounting only for the unit discharge [*D'Agostino*, 2005] might merit further verifications because, after bankfull widths are extracted by means of different techniques [e.g., *Modrick and Georgakakos*, 2014], the kinematic pattern prediction under a selected water discharge would be almost immediate.

The link between the step-to-pool energy dissipation, Manning's *n* calibration and the investigation on several literature formulas for the *U* velocity confirms that the total flow resistance is achieved through different proportions in step pools and transitional reach between plane-bed and step-pool. The spill resistance can be isolated due to the calculation of the local drop dissipation (equation (26)), whereas the total resistance follows a sort of "resistance continuum" (equation (27)) that depends mostly on the statistical relative submergence with respect to the complex bed irregularities (the standard deviation of thalweg elevations), scaled to the overall reach gradient. According to *David et al*. [2010], grain size does not appear to be an adequate measure of roughness in the different channel morphologies, and separate roughness measures need to be used. As also pointed out by *Aberle and Smart* [2003], *Zimmermann* [2010], *David et al*. [2010, 2011], and *Yochum et al*. [2012, 2014], the standard deviation of bed elevation is confirmed in our study to be an excellent primary predictor of the flow resistance, being capable of jointly capturing both grain roughness and bed form roughness.

Whereas, on one hand, the slope is able to directly express the available flow energy, on the other, it contains an opposite signal of energy loss (Figures 4 and 8), which originates from the mountain stream

morphologies but that could also descend from an intrinsic mechanism of greater dissipation in the case of low relative submergence (e.g., increased drag work against the bed protrusions). Although *David et al*. [2010] concluded that the topographical gradient is alone a useful predictor of the relative magnitude of the total resistance, a more correct approach should first check whether the thalweg gradient properly mirrors the bed irregularities and channel morphology of mountain streams. Anthropic actions, channel management, hydraulic works, and condition of the sediment feeding into the channel network might cause an erroneous assessment of the relative resistance patterns.

According to *Wilcox et al*. [2011], most of the energy loss from step to downstream pool results from elevation changes that cause velocity reduction. This occurs particularly in morphologies typical of a steep channel, which have steeper steps with shorter runs and thus a higher elevation difference between the step lip and the pool [*David et al*., 2010]. Our $d_p/\Delta Z$ ratio well reflects the true relative change in elevation, which proved to be excellent in assessing the energy dissipation through the drop. The nonnaturalness of the Vanoi torrent sequences could imply a limitation of validity of equation (26). In fact, the hydraulic conditions of these step-pools are characterized by rapidly varying flow at the step crest, followed by a free hydraulic jump, and gradually varying flow within the pool unit, and the absence of emerged boulders in the transition from pool to next step, which can provide additional sources of dissipation. A further limitation of equation (26) comes from the complex flow patterns along these morphologies making accurate field measurements of critical flow conditions at the natural step crests problematic and prone to uncertainties [*Dust and Wohl*, 2012].

5. Conclusions

During the last decades, the morphology of step pools has been thoroughly investigated with regard to their hydraulics because their hydromorphologic features are too irregular to be precisely associated with a sequence of artificial structures (e.g., a series of straight drop spillways, consolidation check dams, or grade control structures) and too regular to conclude that the synthesis of the overall hydraulic behavior is not predictable. The enhancement of our knowledge is necessary because river restoration proposals for steep streams in environmentally sensitive areas should account as much as possible for the step-pool kinematics. In fact, the correct assessment of flow conditions under different water regimes allows us to improve the design quality in terms of step-pool stability, reduce the overflow hazard, and predict hydrologic effects at the basin outlet (e.g., lag time, flood hydrograph propagation), hydroecological impacts, and interaction between fluid mechanics and sediment transport dynamics.

Although measuring and defining flow depth and flow condition is difficult in steep streams with irregular bed forms [*Rickenamnn and Recking*, 2011], this study has improved and refined certain specific points via experimental research on two real small-scale step-pool units and a transitional reach between plane-bed and step-pool that were built in the Trentino Region (Vanoi torrent) to create fish ladder rings.

The main outcomes of the research, based on data for in-bank flows with water discharges up to approximately 0.2 m^3/s per unit flow width, for pool depth-step height ratios of 0.30–0.85, and slopes in the range 2.6–10.0%, can be summarized as follows.

The divergence between the "at station" mean flow velocity at the step and at the pool exit and that computed as reach-averaged values (U) at the sequence scale is a distinctive characteristic of the energy dissipation. Spill resistance at the lowest discharge ($d_p/\Delta Z$ ratios of approximately 0.3–0.4) occurs and causes dimensionless head losses (ΔE_r) up to 70–80%, which progressively decrease according to equation (26) to 35–40% when the water discharge submerges the step height ($d_p/\Delta Z = 0.85$), as confirmed also by the *Wilcox et al*. [2011] data. The experimental evidence about the energy importance of the relative submergence of the water depth in the pool, which dynamically accounts for maximum/minimum drop height of the step, seems interesting and of practical use in the hydraulic design of stream restoration works. When applying equation (26), d_p can be calculated, given the discharge Q and thus the minimum energy E_s, solving equation (24).

A kind of regime theory equation can be obtained to easily calibrate the U-Q relationships through field measurements. The exponent of the power function was confirmed to be inversely related to the global behavior of the channel reach in terms of energy dissipation over the Q interval under analysis.

Consequently, when Q is constant, a higher reach gradient within the field of steep torrents ($S > 2\%$) does not necessarily mean a greater mean U velocity because the repetition of drops in a step-pool series promotes an overall spill resistance dissipation that greatly exceeds the resistance generated in the gentler slopes (e.g., transitional reach between plane-bed and step-pool).

Both a decreasing relative submergence and an increasing reach slope seem to cooperate in promoting an increment of the energy dissipation in step-pool systems, as expressed by equation (26). The Manning's n prediction through equation (27) as well as the Table 6 data certainly necessitate further verifications (larger number of combinations of channel slopes, reach morphologies and water discharges), but well highlights a threshold from a spill-controlled to a grain-controlled regime of step-pool roughness expressed by the following conditions: $d_m/\sigma_z \approx 1.3$ and $d_m/(\sigma_z\, S) \approx 20$, where the use of the standard deviation (σ_z) of bed elevation is recommended to efficiently represent the overall average roughness height.

Several literature equations have been verified as being valid when computing the reach-averaged U flow velocity within the experimental range of observations. Among these, the specific equations for step-pool and transitional plane-bed/step-pool reaches [*Comiti et al*., 2007; *Ferguson*, 2010; *Zimmermann*, 2010; *Yochum et al*., 2012] have not been found to be significantly more accurate than those that include a wider field of high-roughness morphologies (runs, cascades, or mountain rivers in general), such as the equations proposed by *Rickenmann* [1994], *Aberle and Smart* [2003], *D'Agostino* [2005], and *Rickenmann and Recking* [2011].

Acknowledgments
Field data collection was funded by MIUR—Italian Government: "Ex-60% research projects" 2012–2013 and the Junior Research Grant 2013, CPDR138494 (University of Padova, Vincenzo D'Agostino). The authors are grateful to Gabrielle David reviewer, the two anonymous reviewers, and the Associate Editor Francesco Comiti because their suggestions were supportive to better the manuscript. Users can access the data through an e-mail request to the first author and on the condition that the source of information is declared when data are used.

References

Aberle, J., and G. M. Smart (2003), The influence of roughness structure on flow resistance on steep slopes, *J. Hydraul. Res.*, *41*(3), 259–269, doi:10.1080/00221680309499971.

Abrahams, A. D., G. Li, and J. F. Atkinson (1995), Step-pool streams: Adjustment to maximum flow resistance, *Water Resour. Res.*, *31*(10), 2593–2602, doi:10.1029/95WR01957.

ASCE Task Force (1963), Reports on friction factors on open channels, *J. Hydraul. Div. Am. Soc. Civ. Eng.*, *89*(2), 97–143.

Bathurst, J. C. (1985), Flow resistance estimation in mountain rivers, *J. Hydraul. Eng.*, *111*, 625–643, doi:10.1061/(ASCE)0733-9429(1985)111:4(625).

Bathurst, J. C., D. B. Simons, and R. M. Li (1981), Resistance equation for large-scale roughness, *J. Hydraul. Eng.*, *107*(12), 1593–1613.

Calkins, D., and T. Dunne, (1970), A salt tracing method for measuring channel velocities in small mountain streams, *J. Hydrol.*, *11*, 379–392, doi:10.1016/0022-1694(70)90003-X.

Chen, C. L. (1992), Momentum and energy coefficients based on power law velocity profile, *J. Hydraul. Eng.*, *118*(11), 1571–1584, doi:10.1061/(ASCE)0733-9429(1992)118:11(1571).

Chin, A. (2003), The geomorphic significance of step-pools in mountain streams, *Geomorphology*, *55*(1–4), 125–137, doi:10.1016/S0169-555X(03)00136-3.

Chin, A., and E. Wohl (2005), Toward a theory for step pools in stream channels, *Prog. Phys. Geogr.*, *29*(3), 275–296, doi:10.1191/0309133305pp449ra.

Chin, A., S. Anderson, A. Collison, B. J. Ellis-Sugai, J. P. Haltiner, J. B. Hogervorst, G. M. Kondolf, L. S. O'Hirok, A. H. Purcell, and A. L. Riley (2009), Linking theory and practice for restoration of step-pool streams, *Environ. Manage.*, *43*, 645–661, doi:10.1007/s00267-008-9171-x.

Chow, V. T. (1973), *Open-Channel Hydraulics, International Edition 1973*, McGraw-Hill, Singapore.

Church, M., and A. Zimmermann (2007), Form and stability of step-pool channels: Research progress, *Water Resour. Res.*, *43*, W03415, doi:10.1029/2006WR005037.

Comiti, F., L. Mao, A. Wilcox, E. E. Wohl, and M. A. Lenzi (2007), Field derived relationships for flow velocity and resistance in high-gradient streams, *J. Hydrol.*, *340*(1–2), 48–62, doi:10.1016/j.jhydrol.2007.03.021.

Comiti, F., D. Cadol, and E. E. Wohl (2009), Flow regimes, bed morphology, and flow resistance in self-formed step-pool channels, *Water Resour. Res. 45*, W04424, doi:10.1029/2008WR007259.

Curran, J. H., and E. E. Wohl (2003), Large woody debris and flow resistance in step-pool channels, Cascade Range, Washington, *Geomorphology*, *51*(1–3), 141–157, doi:10.1016/S0169-555X(02)00333-1.

D'Agostino, V. (2004), Sull'affidabilità delle misure di portata nei torrenti montani con il metodo della diluizione salina, in *Proceedings of the 29th Italian Congress of Hydraulics and Hydraulic Structures*, CUDAM, Trento, September 7–10, pp. 1005–1012, BIOS, Cosenza, Italy.

D'Agostino, V. (2005), Velocità media della corrente in torrenti fortemente scabri, in *Proceedings of the Italian Congress AIIA2005*, Associazione Italiana Ingegneria Agraria, June 27–30, Catania, Italy.

D'Agostino, V., and M. A. Lenzi (1998), La massimizzazione della resistenza al flusso nei torrenti con morfologia a step pool, in *Proceedings of the 26th Italian Congress of Hydraulics and Hydraulic Structures*, CUECM, vol. I, pp. 281–293, Catania, Italy.

David, G. C. L., E. Wohl, S. E. Yochum, and B. P. Bledsoe (2010), Controls on spatial variations in flow resistance along steep mountain streams, *Water Resour. Res.*, *46*, W03513, doi:10.1029/2010WR009540.

David, G. C. L., E. Wohl, S. E. Yochum, and B. P. Bledsoe (2011), Comparative analysis of bed resistance partitioning in high-gradient streams, *Water Resour. Res.*, *47*, W07507, doi:10.1029/2010WR009540.

Dingman, S. L. (2007), Comment on "Probabilistic approach to modelling of velocity distributions in fluid flows" by C.-L. Chiu and S.-M. Hsu, *J. Hydrol.*, *316*, 28–42. *J. Hydrol.*, *335*(3–4), 419–428, doi:10.1016/j.jhydrol.2006.09.006.

Dust, D., and E. E. Wohl (2012), Characterization of the hydraulics at natural step crests in step-pool streams via weir flow concepts, *Water Resour. Res.*, *48*, W09542, doi:10.1029/2011wr011724.

Einstein, H. A., and N. L. Barbarossa (1952), River channel roughness, *Transactions of the ASCE*, *117*, 1121–1132.

Ferguson, R. (2007), Flow resistance equations for gravel- and boulder-bed streams, *Water Resour. Res.*, *43*, W05427, doi:10.1029/2006WR005422.

Ferguson, R. (2010), Time to abandon the Manning equation?, *Earth Surf. Processes Landforms*, *35*(15), 1873–1876, doi:10.1002/esp. 2091.
Guo, J. (2002), Logarithmic matching and its applications in computational hydraulics and sediment transport, *J. Hydraul. Res.*, *40*(5), 555–564, doi:10.1080/00221680209499900.
Henderson, F. M. (1966), *Open Channel Flow*, pp. 87–103, MacMillan Co, N. Y.
Indri, E. (1942), Misure sulla velocità dell'acqua in alvei montani a forte scabrezza, *L'Acqua*, *20*(9), 113–121.
Jarrett, R. D. (1984), Hydraulics of high-gradient streams, *J. Hydraul. Eng.*, *110*(11), 1519–1539, doi:10.1061/(ASCE)0733-9429(1984)110:11(1519).
Judd, H. E., and D. F. Peterson (1969), Hydraulics of large bed element channels, *Rep. PRWG17-6*, Utah Water Res. Lab., Utah State Univ.
Kaufmann, P. R. (1987), Channel morphology and hydraulic characteristics of torrent-impacted forest streams in the Oregon Coast Range USA, PhD dissertation, Oregon State Univ., Corvallis, Oreg.
Kaufmann, P. R., J. M. Faustini, D. P. Larsen, and M. A. Shirazi (2008), A roughness-corrected index of relative bed stability for regional stream surveys. *Geomorphology*, *99*(1), 150–170, doi:10.1016/j.geomorph.2007.10.007.
Kean, J. W., and J. D. Smith (2006), Form drag in rivers due to small-scale natural topographic features: 2. Irregular sequences, *J. Geophys. Res.*, *111*, F04010, doi:10.1029/2006JF000490.
Keller, E. A., and F. J. Swanson (1979), Effects of large organic material on channel form and fluvial processes, *Earth Surf. Processes Landforms*, *4*(4), 361–380.
Lee, A. J., and R. I. Ferguson (2002), Velocity and flow resistance in step-pool streams, *Geomorphology*, *46*(1), 59–71, doi:10.1016/S0169-555X (02)00054-5.
Lenzi, M. A., V. D'Agostino, and D. Sonda (2000), Ricostruzione morfologica e recupero ambientale dei torrenti. Criteri metodologici ed esecutivi, BIOS, 208 pp., Cosenza, Italy.
Limerinos, J. T. (1970), Determination of the Manning Coefficient from Measured Bed Roughness in *Natural Channels, Water Supply Paper* 1898-B, United State Geological Survey, 47 pp., Washington, D. C.
MacFarlane, W. A., and E. E. Wohl (2003), Influence of step composition on step geometry and flow resistance in step-pool streams of the Washington Cascades, *Water Resour. Res.*, *39*(2), 1037, doi:10.1029/2001WR001238.
Marcus, W. A., K. Roberts, L. Harvey, and G. Tackman (1992), An evaluation of methods for estimating Manning's n in small mountain streams, *Mt. Res. Dev.*, *12*(3), 227–239, doi:10.2307/3673667.
Millar, R. G. (1999), Grain and form resistance in gravel-bed rivers, *J. Hydraul. Res.*, *37*(3), 303–312, doi:10.1080/00221686.1999.9628249.
Montgomery, D. R., and J. M. Buffington (1997), Channel-reach morphology in mountain drainage basins, *Geol. Soc. Am. Bull.*, *109*(5), 596–611, doi:10.1130/0016-7606(1997)109<0596:CRMIMD>2.3.CO;2.
Modrick, T. M., and K. P. Georgakakos (2014), Regional bankfull geometry relationships for southern California mountain streams and hydrologic applications, *Geomorphology*, *221*, 242–260, doi:10.1016/j.geomorph.2014.06.004.
Pagliara, S., and P. Chiavaccini (2006), Flow resistance of rock chutes with protruding boulders, *J. Hydraul. Eng.*, *132*(6), 545–552, doi:10.1061/(ASCE)0733-9429(2006)132:6(545).
Parker, G., and A. W. Peterson (1980), Bar resistance of gravel-bed streams, *J. Hydraul. Div. Am. Soc. Civ. Eng.*, *106*, 1559–1575.
Pasternack, G. B., C. R. Ellis, K. A. Leier, B. L. Vallé, and J. D. Marr (2006), Convergent hydraulics at horseshoe steps in bedrock rivers, *Geomorphology*, *82*(1-2), 126–145, doi:10.1016/j.geomorph.2005.08.022.
Peterson, D. F., and P. K. Mohanty (1960), Flume studies of flow in steep, rough channels, *J. Hydraul. Div. Am. Soc. Civ. Eng.*, *86*, 55–76.
Rajaratnam, N., and R. K. MacDougall (1983), Erosion by plane wall jets with minimum tailwater, *J. Hydraul. Eng.*, *109*(7), 1061–1064, doi:10.1061/(asce)0733-9429(1983)109:7(1061).
Rajaratnam, N., and M. R. Chamani (1995), Energy loss at drops, *J. Hydraul. Res.*, *33*(3), 373–384, doi:10.1080/00221689509498578.
Reid, D. E., and E. J. Hickin (2008), Flow resistance in steep mountain streams, *Earth Surf. Processes Landforms*, *33*(14), 2211–2240, doi:10.1002/esp.1682.
Rickenmann, D. (1991), Hyperconcentrated flow and sediment transport at steep slopes. *J. Hydraul. Eng.*, *117*(11), 1419–1439.
Rickenmann, D. (1994), An alternative equation for the mean velocity in gravel-bed rivers and mountain torrents, in *Proceedings ASCE 1994 National Conference on Hydraulic Engineering*, Buffalo, N. Y., USA, edited by G. V. Cotroneo and R. R. Rumer, vol. 1, pp. 672–676, Reston, Va.
Rickenmann, D., and A. Recking (2011), Evaluation of flow resistance in gravel-bed rivers through a large field data set, *Water Resour. Res.*, *47*, W07538, doi:10.1029/2010WR009793.
Roberson, J. A., and C. T. Crowe (1997), *Engineering Fluid Mechanics*, 6th ed., John Wiley, N. Y.
Smart, G. M. (1999), Turbulent velocity profiles and boundary shear in gravel bed rivers, *J. Hydraul. Eng.*, *125*(2), 106–116, doi:10.1061/(asce)0733-9429(1999)125:2(106).
Whittaker, J. G., and M. N. Jaeggi (1982), Origin of step-pool systems in mountain streams, *J. Hydraul. Div. Am. Soc. Civ. Eng.*, *108*, 758–773.
Wilcox, A. C., and E. E. Wohl (2007), Field measurements of three-dimensional hydraulics in a step–pool channel, *Geomorphology*, *83*(3-4), 215–231, doi:10.1016/j.geomorph.2006.02.017.
Wilcox, A. C., J. M. Nelson, and E. E. Wohl (2006), Flow resistance dynamics in step-pool channels: 2. Partitioning between grain, spill, and woody debris resistance, *Water Resour. Res.*, *42*, W05418, doi:10.1029/2005WR004278.
Wilcox, A. C., E. E. Wohl, F. Comiti, and L. Mao (2011), Hydraulics, morphology, and energy dissipation in an alpine step-pool channel, *Water Resour. Res.*, *47*, W07514, doi:10.1029/2010WR010192.
Wohl, E. E., and D. M. Thompson (2000), Velocity characteristics along a small step–pool channel, *Earth Surf. Processes Landforms*, *25*(4), 353–367, doi:10.1002/(SICI)1096-9837(200004)25:4<353::AID-ESP59>3.0.CO;2-5.
Wyrick, J. R., and G. B. Pasternack (2008), Modeling energy dissipation and hydraulic jump regime responses to channel nonuniformity at river steps, *J. Geophys. Res.*, *113*, F03003, doi:10.1029/2007JF000873.
Yochum, S. E., Bledsoe, B. P., David, G. C., and Wohl, E. (2012), Velocity prediction in high-gradient channels, *J. Hydrol.*, *424*, 84–98, doi:10.1016/j.jhydrol.2011.12.031.
Yochum, S. E., B. P. Bledsoe, E. Wohl, and G. C. L. David (2014), Spatial characterization of roughness elements in high-gradient channels of the Fraser Experimental Forest, Colorado, USA, *Water Resour. Res.*, *50*, 6015–6029, doi:10.1002/2014WR015587.
Zimmermann, A. (2010), Flow resistance in steep streams: An experimental study, *Water Resour. Res.*, *46*, W09536, doi:10.1029/2009WR007913.
Zimmermann, A., and M. Church (2001), Channel morphology, gradient profiles and bed stresses during flood in a step-pool channel, *Geomorphology*, *40*(3-4), 311–327, doi:10.1016/S0169-555X(01)00057-5.